Thin Solid Films 535 (2013) 83–87

Contents lists available at SciVerse ScienceDirect

Thin Solid Films

journal homepage: www.elsevier.com/locate/tsf

HCl and Br_2-MeOH etching of $Cu_2ZnSnSe_4$ polycrystalline absorbers

Marina Mousel [a,*], Alex Redinger [a], Rabie Djemour [a], Monika Arasimowicz [a], Nathalie Valle [b], Phillip Dale [a], Susanne Siebentritt [a]

[a] University of Luxembourg, Laboratory for Photovoltaics, 41, rue du Brill, L-4422 Belvaux, Luxembourg
[b] CRP Gabriel Lippmann, 41, rue du Brill, L-4422 Belvaux, Luxembourg

ARTICLE INFO

Available online 7 January 2013

Keywords:
CZTSe
Absorber
Bromine
HCl
ZnSe
CTSe
Efficiency

ABSTRACT

$Cu_2ZnSnSe_4$ solar cells made from absorbers etched in HCl and Br in methanol (Br_2-MeOH) are studied. The absorbers show surface compositions, different from bulk compositions, as revealed by secondary ion mass spectrometry (SIMS) depth profiles. They indicate the presence of secondary phases where the most prominent are a Zn related phase and a Cu, Sn related phase. The secondary phases can be removed by etching in HCl or Br_2-MeOH. The absorbers are analyzed before and after etching by scanning electron microscopy and SIMS, and solar cells by current–voltage measurements. These results indicate that the Cu, Sn related phase is strongly detrimental to solar cell devices by reducing drastically open-circuit voltage (V_{OC}) and fill factor (FF) and is etched by Br_2-MeOH, but not by HCl. In fact solar cell results improved from about 4% to above 5%. All solar cell parameters improved slightly for HCl etching but for Br_2-MeOH etching we observe a significant increase of V_{OC} and FF. An efficiency of 5% was obtained in both cases and 5.8% efficiency is the best device obtained after Br_2-MeOH etching.

1. Introduction

$Cu_2ZnSn(S,Se)_4$ (CZTS(e)) absorbers for photovoltaic applications gain more and more interest in thin film solar cell research and have already achieved 10.1% efficiency [1]. Considering their direct band gap [2], high absorption coefficient and abundance of raw materials, they present a promising alternative to existing thin film solar cell technologies. It is well known that the existence region of pure CZTS(e) is much smaller compared with that of $Cu(In,Ga)(S,Se)_2$ (CIGS(e)) material [3] and thus the formation of detrimental secondary phases is a challenging issue for $Cu_2ZnSn(S,Se)_4$ based solar cells. Current knowledge places the more efficient devices in the Cu-poor and in the slightly Zn-rich region [4]. However, even in this region, secondary phases are very likely and probably detrimental, thus limiting solar cell efficiencies. The most prominent secondary phases are the ternary Cu_2SnSe_3 and the ZnSe phases. The presence of secondary phases at the interfaces has already been reported in literature for CZTS [5,6] and CZTSe [7–9] systems. Detrimental ZnSe secondary phase at the back contact has been observed by S. Ahn et al. [7] and by A. Redinger et al. [8] and recently J.T. Wätjen et al. [9] and A. Redinger et al. [10] showed direct evidence of detrimental ZnSe at the interface. In fact, the heterojunction interface is still a limiting factor in CZTSSe solar cells since most devices exhibit dominant interface recombination [11]. In order to improve the heterojunction interface chemical etching methods can be used to remove detrimental secondary phases.

In this regard Timmo et al. [12] studied chemical surface treatment on monograin powders using several etchants such as HCl and Br_2-MeOH. Although chemical etching has been less studied for CZTS(e) absorbers compared with CIGS(e) (see for example [13]) it is clear that bromine solutions are efficient etchants. Bromine etching results in a global flattening of the initial surface providing a non-selective thinning of the absorber [13]. Moreover it was shown that surface compositions stay constant during the etching process in the case of CIGSe. In this paper, we studied surface etching with HCl and Br_2-MeOH of CZTSe polycrystalline absorbers with respect to secondary phases and solar cell parameters.

2. Experimental details

The CZTSe polycrystalline absorbers were produced by a precursor-annealing process. First all the elements (Cu, Zn, Sn and Se) were co-evaporated at 320 °C onto a molybdenum coated soda lime glass in a molecular beam epitaxy system as described elsewhere [14]. Precursors with different compositions were obtained by tuning the fluxes of the elements. The precursors were then annealed for 30 min in a tube furnace at 500 °C in an H_2/N_2 atmosphere with 10^2 Pa total pressure. To avoid decomposition of the CZTSe during the final heat treatment, the films were annealed in an SnSe and Se atmosphere provided in form of powders in the graphite box (for further details see [15]). After the annealing some of the absorbers were etched for 1 min either with concentrated (37 wt.%) HCl or with 0.02 M bromine methanol (Br_2-MeOH). The morphology and the composition before and after etching were analyzed by scanning electron microscopy (SEM) and by 20 keV energy-dispersive X-ray spectroscopy (EDX). The compositions

* Corresponding author.
E-mail address: marina.mousel@uni.lu (M. Mousel).

0040-6090/$ – see front matter
http://dx.doi.org/10.1016/j.tsf.2012.12.095

of the precursors were varied from Cu/(Zn + Sn) = 0.8 to 1.6 and from Zn/Sn = 0.7 to 1.7. Secondary ion mass spectrometry (SIMS) depth profile measurements were performed on the absorbers with Cs^+-ions and positively charged Cs-metal clusters have been detected. The element intensities of the SIMS measurements are normalized to the middle of the absorber in order to highlight changes compared with the bulk.

In order to remove a possible Cu_xSe secondary phase, all the annealed samples were etched in 5 wt.% KCN for 30 s as standard procedure. After depositing the CdS buffer layer by chemical bath deposition, the window deposition was performed by magnetron sputtering of i-ZnO and Al-doped ZnO. At last, an Ni-Al grid was deposited by e-beam evaporation for front contacting. The typical size for the solar cells is 0.5 cm^2 total area. The solar cell parameters were determined using a current–voltage (I–V) measurement set-up equipped with a halogen lamp which has been adjusted to 100 mW/cm^2. Further solar cell parameters have been extracted with J.R. Sites et al.'s [16] method.

3. Results and discussion

Fig. 1 shows the sample compositions as determined by EDX plotted in the phase diagram adapted from I.V. Dudchak and L. Piskach [17] as precursors and after annealing. In order to be able to represent the compositions of the samples in the phase diagram, the Se content was assumed to be stoichiometric. Although a relatively broad region of the phase diagram around the single phase $Cu_2ZnSnSe_4$ existence region has been prepared via coevaporation, after the annealing the compositions shift significantly and the final film compositions are always situated on the Cu_2SnSe_3–$Cu_2ZnSnSe_4$ and on the ZnSe–$Cu_2ZnSnSe_4$ tie lines. From that figure it is suggested that for this set of samples we have either the ternary Cu_2SnSe_3, or the binary ZnSe as secondary phases in the absorber.

The best absorber layers gave an efficiency of around 4% when the composition was Cu-poor and Zn-rich. Although the composition of the absorbers changed after annealing there was a clear correlation between solar cell efficiency and precursor composition. The precursor compositions close to Cu-poor and Zn-rich gave the best results as absorbers whereas Cu-rich and Sn-rich precursors did not lead to working devices. Moreover SIMS depth profile measurements performed on the absorbers indicate a clear trend of two different profiles related to the efficiency of the solar cells. Two typical examples of those SIMS depth profiles are depicted in Fig. 2. The solar cells with an efficiency above 4% (Fig. 2(a)) show a depth profile where the Zn ratio at the surface is higher than in the bulk. The low efficiency or non-working solar cells exhibit SIMS depth profiles similar to the one shown in Fig. 2(b). These depth profiles have in common that the Zn content at the interface decreases compared with that in the bulk. Moreover the Cu and Sn contents are slightly increased in the first few hundred nanometers of the absorber compared with the rest of the film. Finally the Cu-content very close to the heterojunction strongly decreases. Additionally it has to be pointed out that Cu and Sn profiles in all SIMS measurements vary together over almost all the absorber depth. The Zn increase at the back occurring in most of the SIMS profiles is in agreement with a ZnSe phase at the back contact [8].

This shows that we have different compositions at the surface than in the bulk which could not necessarily be determined via integral composition measurements. Moreover the different compositions at the surface can be related to secondary phases. The Cu and Sn related phase strongly inhibits solar cell devices. It is safe to assume that the profiles in Fig. 2(a) indicate a ZnSe phase at the surface, and the profiles in Fig. 2(b) a ternary Cu_2SnSe_3 phase. Although the ternary Cu_2SnSe_3 phase has not been directly measured, this phase presents a lower band gap of 0.84 eV [18] which will result in a strongly reduced open-circuit voltage (V_{OC}). This lower V_{OC} was observed in the set of solar cells in correlation with the Cu, Sn related phases at the surface in the SIMS profiles. Both secondary phases are detrimental to solar cell devices. The ternary due to its lower band gap leads to increased recombination, while the ZnSe phase limits the current, as shown recently [9]. However HCl solutions have successfully been employed by H. Tamura et al. [19] to etch ZnSe crystals. Bromine solutions are known to be efficient etchants and were used to reduce the thickness of CIGSe absorbers

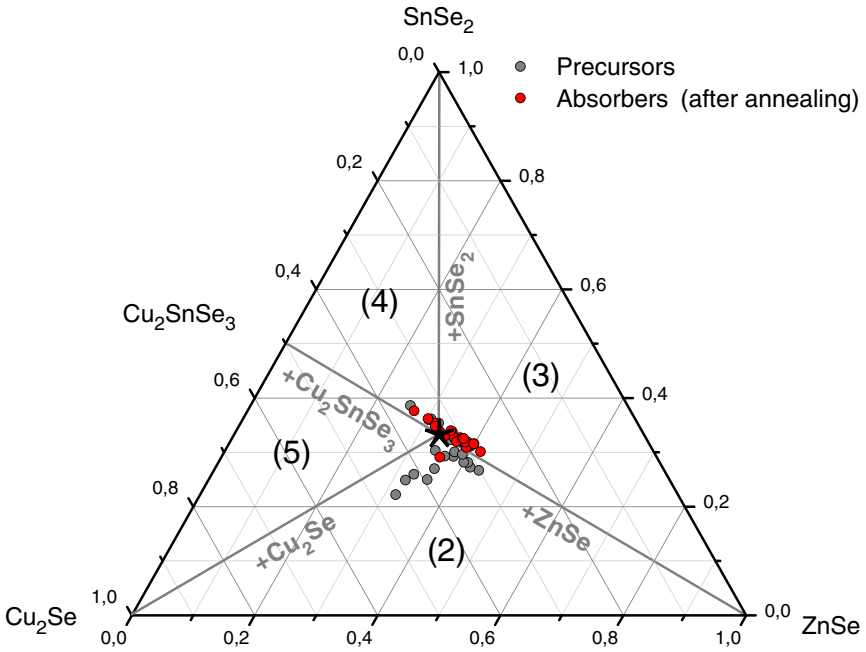

Fig. 1. Sample compositions plotted in the phase diagram adapted from [17] as precursor (gray dots) and after annealing (red dots). The different regions of the phase diagram (★) $Cu_2ZnSnSe_4$, (2) $Cu_2ZnSnSe_4 + Cu_2Se + ZnSe$, (3) $Cu_2ZnSnSe_4 + SnSe_2 + ZnSe$, (4) $Cu_2ZnSnSe_4 + Cu_2SnSe_3 + SnSe_2$ and (5) $Cu_2ZnSnSe_4 + Cu_2SnSe_3 + Cu_2Se$ represent the existence region of $Cu_2ZnSnSe_4$ and secondary phases. The tie lines represent the regions where $Cu_2ZnSnSe_4$ and one other secondary phase are present as indicated in the graph.

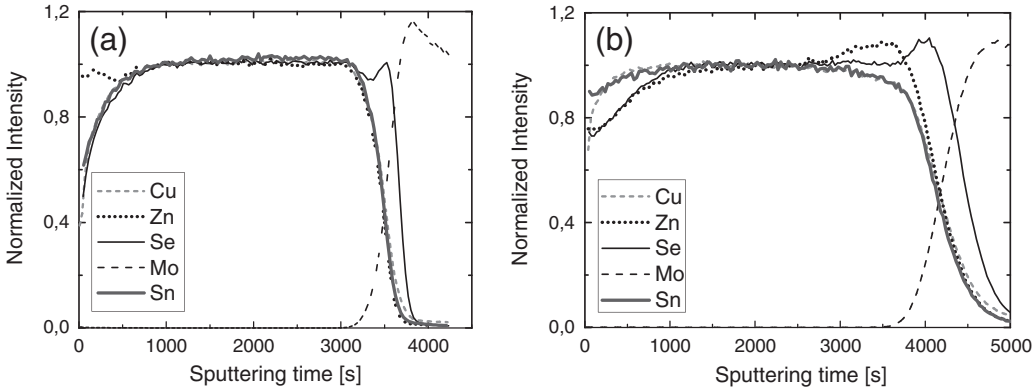

Fig. 2. Two SIMS depth profiles of unetched absorbers for (a) absorber that gave a solar cell efficiency higher than 4% and (b) absorber that gave no working solar cell.

[13]. Thus Br_2-MeOH is used as a non-selective etchant which will remove the ternary if present.

HCl etching was performed on samples that showed a Zn-rich and Cu-poor composition (Zn/Sn = 1.11, Cu/(Zn + Sn) = 0.93 and Cu/Sn = 1.97) and a SIMS depth profile like that shown in Fig. 2(a). SEM cross-sections of two absorbers (Fig. 3) before and after HCl etching suggest that HCl is removing a secondary phase. Fig. 3(a) shows a possible phase segregation on top of the absorber (smaller grains on top of the surface in the SEM micrograph (a)) while in Fig. 3(b) this phase segregation seems to be removed or at least minimized. In addition to the SIMS profiles discussed above Fig. 4 depicts a comparison between absorbers before and after etching for both etchants, HCl and Br_2-MeOH. In Fig. 4(a) and (b) the same absorber was analyzed before and after HCl etching. The Zn profile changes after etching. At the surface the Zn ratio decreases compared with the bulk and the profile of the unetched absorber (Fig. 4(a)). These measurements agree with the results given in [19] which showed that acidic solutions remove a Zn related secondary phase.

Fig. 4(c) and 4(d) show SIMS profiles of an absorber before and after etching with Br_2-MeOH. The profiles are getting flatter at the surface after the Br_2-MeOH etching. There is no more a decrease of the Zn ratio or an increase of the Cu and Sn ratios towards the surface. These observations are valid for all absorbers treated with Br_2-MeOH and strongly corroborate the model of a Cu, Sn related phase at the near surface region which could be at least partially removed by Br_2-MeOH.

In the following, we discuss the solar cells resulting from etched and unetched absorbers. The current density–voltage (J–V) curves given for one absorber are typical for a set of 6 solar cells. As already mentioned before, the samples of Fig. 1 without any surface treatment besides the KCN etching, with compositions of slightly Cu-poor and Zn-rich gave solar cell efficiencies above 4% on a regular basis. The effect of KCN etching is not studied in this work, but see for example [20,21] to get insights of KCN etching on CZTS absorbers. The solar cells made from absorbers that were etched improved significantly. 5% efficiency (η) was achieved with both etchants, whereas 5.8% could be achieved with Br_2-MeOH. The (J–V) curves for solar cells whose absorbers were treated with the two different etchants are shown in Fig. 5. While the absorber etched with HCl improved slightly in all solar cell parameters, the J–V curve under illumination of the Br_2-MeOH etched absorber shows significant improvements of the fill factor (FF) and V_{OC} in agreement with the strong decrease in the saturation current (J_0) and the decrease in the diode factor. The parasitic resistances are not affected by the etching in both cases.

In addition it has to be pointed out that the solar cell parameters for absorbers etched with Br_2-MeOH seem to depend on the composition of the precursors (see Tables 1 and 2). In fact samples III and IV gave the best solar cell devices. They significantly improved (from 0.5% to 5.8% and from 3.3% to 5.4%) and this can be understood while looking at the compositions of the precursors. They were Cu-rich regarding the Cu/Sn ratio (Cu/Sn > 2) in contrast to sample V. Because of the high Cu content they could potentially form more ternary on top during the annealing in an SnSe atmosphere. Therefore the V_{OC} of unetched devices is very low. Br_2-MeOH could remove the ternary and thereby remove one of the detrimental secondary phases which inhibits solar cell device efficiency.

4. Conclusions

From the observations described above it is clear that HCl and Br_2-MeOH improve solar cell devices by removing secondary phases. The phase diagram, EDX measurements and SEM cross-sections imply Cu_2SnSe_3 and ZnSe as most likely prominent detrimental secondary phases. From SIMS measurements it appears that the detrimental secondary phases are located at the surface and that etching either with HCl or Br_2-MeOH could at least partially remove them improving the surface. Solar cell J–V curves showed that the device parameters could be improved, especially V_{OC} by Br_2-MeOH treatment. This is possibly due to the ternary Cu_2SnSe_3 formation on top even for standard compositions (Cu/(Zn + Sn) < 1) which strongly inhibit working devices. Efficiencies above 5% have been achieved with both HCl and Br_2-MeOH etchants although Br_2-MeOH is more suitable to remove the Cu, Sn related phase. 5.8% efficiency has been achieved with Br_2-MeOH etched absorbers.

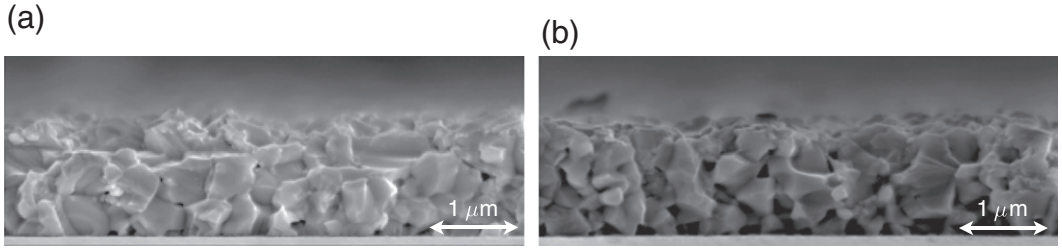

Fig. 3. SEM cross-sections of sample I (a) without etching and (b) after 1 min HCl etching.

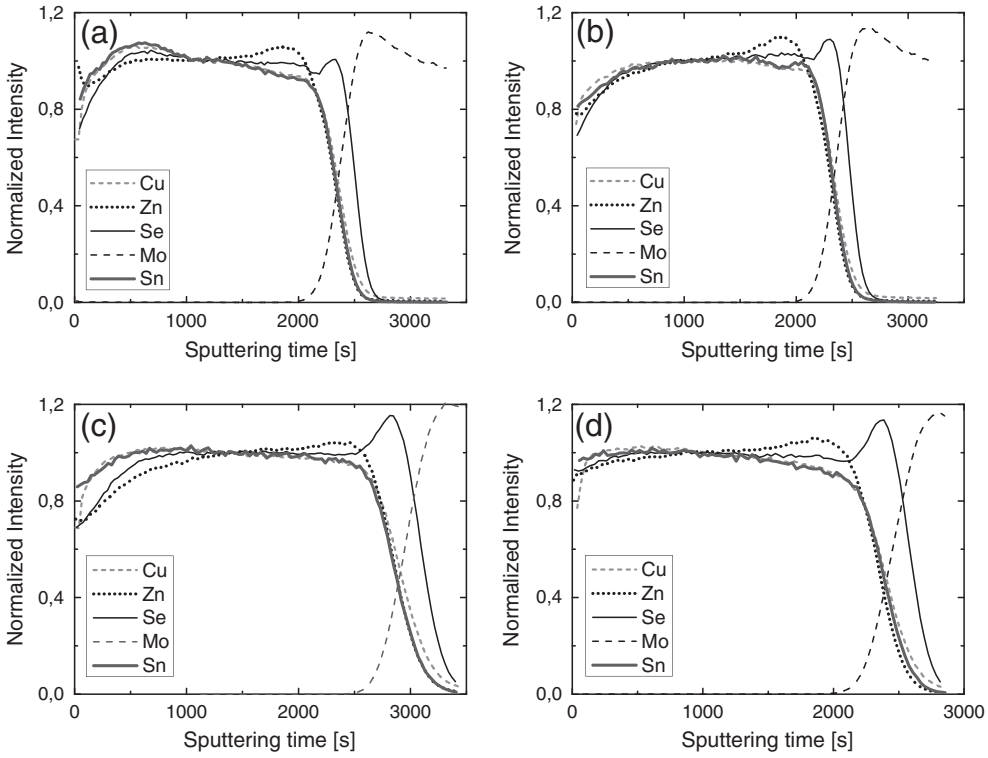

Fig. 4. Different SIMS depth profiles for two different absorbers I and II: (a) absorber I without etching, (b) absorber I after HCl etching, (c) absorber II without etching, and (d) absorber II after Br_2-MeOH etching.

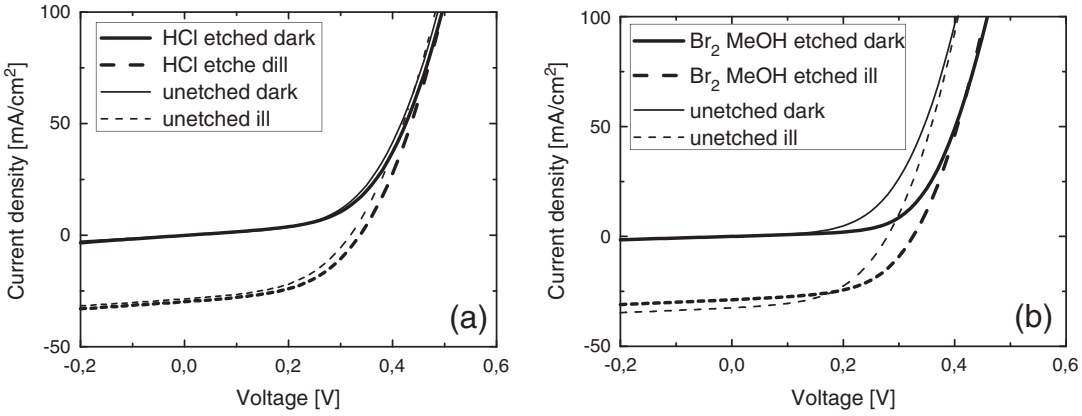

	Unetched	HCl	Unetched	Br_2-MeOH
η [%]	4.4	5.0	4.6	5.1
V_{OC} [mV]	319	337	279	325
J_{SC} [mA/cm^2]	28.5	29.8	32.5	28.8
FF [%]	49	50	50	54
R_s [Ωcm^2]	0.6	0.6	0.5	0.5
G_{Sh} [mS/cm^2]	15	16	11	11
A	2.3	2.2	2	1.8
J_0 [mA/cm^2]	$1.4\ 10^{-1}$	$9.3\ 10^{-2}$	$1.9\ 10^{-1}$	$2.9\ 10^{-2}$

Fig. 5. J–V curves in the dark and under illumination from solar cells made from (a) unetched sample I, and same absorber I etched with HCl and (b) unetched sample II and the same absorber II etched with Br_2-MeOH.

Table 1
20 keV EDX values for precursors of absorbers which were etched afterwards with Br_2-MeOH.

Samples	Zn/Sn	Cu/(Zn + Sn)	Cu/Sn
III	1.24	1.05	2.35
IV	1.33	0.91	2.13
V	1.16	0.84	1.82

Table 2
Solar cell parameters for absorbers with different precursor compositions before and after Br_2-MeOH etching.

Samples	Etchants	V_{OC} [mV]	η [%]	J_{SC} [mA/cm^2]	FF [%]
III	Without	137	0.5	13.5	28
III	Br_2-MeOH	338	5.8	35.4	49
IV	Without	261	3.3	28.3	45
IV	Br_2-MeOH	324	5.4	32.7	51
V	Without	345	4.3	23.5	53
V	Br_2-MeOH	324	4.8	28.2	53

Acknowledgments

The authors acknowledge FNR Luxembourg for funding through the project Nr. C08/MS/20, Bosch GmbH, TDK Corporation in the framework of the TDK Europe Professorship and M. Kurihara at TDK Corporation for solar cell finishing.

References

[1] D.A.R. Barkhouse, O. Gunawan, T. Gokmen, T.K. Todorov, D.B. Mitzi, Prog. Photovolt. Res. Appl. 20 (2012) 6.
[2] L. Gütay, A. Redinger, R. Djemour, S. Siebentritt, Appl. Phys. Lett. 100 (2012) 102113.
[3] S. Siebentritt, S. Schorr, Prog. Photovolt. Res. Appl. 20 (2012) 512.
[4] H. Katagiri, K. Jimbo, M. Tahara, H. Araki, K. Oishi, MRS Proc. 1165 (2011) 125.
[5] K. Wang, B. Shin, K.B. Reuter, T. Todorov, D.B. Mitzi, S. Guha, Appl. Phys. Lett. 98 (2011) 051912.
[6] C. Platzer-Björkman, J. Scragg, H. Flammersberger, T. Kubart, M. Edoff, Sol. Energy Mater. Sol. Cells 98 (2012) 110.
[7] S. Ahn, S. Jung, J. Gwak, A. Cho, K. Shin, K. Yoon, D. Park, H. Cheong, J.H. Yun, Appl. Phys. Lett. 97 (2010) 021905.
[8] A. Redinger, K. Hones, X. Fontané, V. Izquierdo-Roca, E. Saucedo, N. Valle, A. Perez-Rodríguez, S. Siebentritt, Appl. Phys. Lett. 98 (2011) 101907.
[9] J. Timo Wätjen, J. Engman, M. Edoff, C. Platzer-Björkman, Appl. Phys. Lett. 100 (2012) 173510.
[10] A. Redinger, D.M. Berg, P.J. Dale, R. Djemour, L. Gütay, T. Eisenbarth, N. Valle, S. Siebentritt, IEEE J. Photovolt. 1 (2011) 200.
[11] D.B. Mitzi, O. Gunawan, T.K. Todorov, K. Wang, S. Guha, Sol. Energy Mater. Sol. Cells 95 (2011) 1421.
[12] K. Timmo, M. Altosaar, J. Raudoja, M. Grossberg, M. Danilson, O. Volobujeva, E. Mellikov, 2010 35th IEEE Photovoltaic Specialists Conference, IEEE, 2010, p. 001982.
[13] M. Bouttemy, P. Tran-Van, I. Gerard, T. Hildebrandt, A. Causier, J. Pelouard, G. Dagher, Z. Jehl, N. Naghavi, G. Voorwinden, B. Dimmler, M. Powalla, J. Guillemoles, D. Lincot, A. Etcheberry, Thin Solid Films 519 (2011) 7207.
[14] A. Redinger, S. Siebentritt, Appl. Phys. Lett. 97 (2010) 092111.
[15] A. Redinger, D.M. Berg, P.J. Dale, S. Siebentritt, J. Am. Chem. Soc. 133 (2011) 3320.
[16] J. Sites, P. Mauk, Sol. Cells 27 (1989) 411.
[17] I. Dudchak, L. Piskach, J. Alloys Compd. 351 (2003) 145.
[18] G. Marcano, C. Rincón, L.M. de Chalbaud, D.B. Bracho, G.S. Pérez, J. Appl. Phys. 90 (2001) 1847.
[19] H. Tamura, Y. Okuno, H. Kato, J. Electron. Mater. 23 (1994) 835.
[20] M. Bär, B.-A. Schubert, B. Marsen, R.G. Wilks, S. Pookpanratana, M. Blum, S. Krause, T. Unold, W. Yang, L. Weinhardt, C. Heske, H.-W. Schock, Appl. Phys. Lett. 99 (2011) 222105.
[21] M. Bär, B.-A. Schubert, B. Marsen, S. Krause, S. Pookpanratana, T. Unold, L. Weinhardt, C. Heske, H.-W. Schock, Appl. Phys. Lett. 99 (2011) 152111.